

An Alternative Model of Overshot Waterwheel Based on a Tracking Nozzle Angle Technique for Hydropower Converter

Lie Jasa*[†], Ardyono Priyadi**[‡], Mauridhi Hery Purnomo**[‡]

*Department of Electrical Engineering, Faculty of Engineering, Udayana University, Denpasar, Bali, Indonesia

**Department of Electrical Engineering, Faculty of Technology Industry, Sepuluh Nopember Institute of Technology, Surabaya, Indonesia

(liejasa@unud.ac.id, priyadi@ee.its.ac.id, hery@ee.its.ac.id)

[‡]Corresponding Author; Mauridhi Hery Purnomo, Department of Electrical Engineering, Kampus ITS Sukolilo, Surabaya 60111, Indonesia, Tel: +62 31 594 7302, Fax: +62 31 593 1237, hery@ee.its.ac.id

Received: 25.09.2014 Accepted: 09.11.2014

Abstract- The efficiency of a waterwheel is a measure of its capacity to convert the kinetic energy of flowing water into mechanical energy. The rotation of a waterwheel is influenced by several parameters including blade shape, number of blades, nozzle angle, and rim diameter. This study focuses on finding the parameters that influence the rotations per minute (RPM) of the waterwheel. The research method involved analysis, modelling, and a validation step. The results show that the triangular blade was an improvement over previous research on waterwheels with propeller blades. Our experiments produced 5,73 higher efficiency than a vane having a nozzle angle θ of 20° .

Keywords- Waterwheel, RPM, blade, nozzle.

1. Introduction

Global warming is a great concern to Indonesian people[1]. More sustainable practices require the use of clean energy sources. Achieving sustainable energy use requires everyone to use energy wisely, and in a way friendly to the environment. The developments of renewable energy sources are necessary[2] because: (a) oil prices are unstable and (b) mineral-based energy reserves are limited.

Hydroelectricity is an important component of the world's renewable energy supply. In 2011, hydroelectricity accounted for 15% of the world electricity production[3],[4] Among all renewable energy sources, water has the lowest cost and is the most reliable resource. Micro-hydro is popular because of its simple design, easy operation, and inexpensive installation[5]. Recent research of micro-hydro used a waterwheel in Dusun Gambuk Pupuan Tabanan Bali, Indonesia[6],[7],[8] to produce only 0,7 kW of energy. It is possible that the waterwheel was inefficient because it was unable to convert the maximum amount of water energy. The parameters of the waterwheel included a head of 17 m, a water discharge of 40 L/sec, 23–26 rotations per minute (RPM), and a diameter of 200 Cm, which should produce more than 0,7 kW[9].

Hydropower systems are classified, in accordance with their installation capacities, as large, medium-size, small, and micro[10]. Micro-hydro systems generally have a generating capacity of less than 100 kW. The capacity of power generation is determined by the ability of the waterwheel to convert the water's kinetic energy into mechanical energy. Physicists generally describe waterwheels as analogous to physical, biological systems[11],[12],[13],[14]. Flowing water flow has a capacity of energy, and the waterwheel converts the kinetic energy of flowing water to generate electricity. This study focuses on finding the parameters of the waterwheel to produce a maximum RPM.

Research on hydropower converters show that some parameters of the waterwheel design have great impact on efficiency[15],[16]. Rotation of a waterwheel depends on the radius, blade, water discharge, volume, and nozzle angle[17] The volume of the blade is affected by gravitational force, causing the waterwheel to rotate clockwise. The speed of the waterwheel is measured in RPM, whereas the radius of the waterwheel determines the torque produced.

Previous research examined the overshot waterwheel [15], including the analysis of physical and mathematical models. In this study, the authors analyzed an overshot waterwheel of

cross-flow turbine with mathematical models, especially looking at the flow in the space between each blade, conducted simulation of the model, made a prototype of the waterwheel, and compared efficiency with previous research. A waterwheel prototype was developed with an adjustable nozzle length, nozzle position, and nozzle angle. The highest RPM of the waterwheel is determined by adjusting these parameters.

Propeller blade design developed by Denny[15] was compared with our model. Both prototypes of the models were developed with equal diameter, blade thickness, and blade number. The purpose was to obtain real data for both models. The technical results proved that our model was able to produce higher RPM.

2. Design Overshot Waterwheels

2.1. Previous Model

The ideal overshoot waterwheel[15] model has 12 triangular buckets attached to the wheel rim. Each bucket moves freely on the horizontal axis. Buckets are filled with water that drops vertically through the channel. The water-filled bucket causes the waterwheel to spin. Low spill angles, ϕ_1 , near the rim of the wheel cause the buckets to shed water; otherwise, no water is spilled. It was assumed that the wheel is frictionless and works by turning a millstone. The difference between the ideal waterwheels and the real waterwheels is in the mathematical analysis and physics, whereby an ideal waterwheel does not exist. First, real waterwheels did not have pivoted buckets. This design was adopted to ensure that water does not spill out as the wheel turned. Instead, the rim of the wheel is partitioned off into sections rotating with the wheel, and so the amount of water spilled out increases as the spill angle (ϕ) increases[15]. As the wheel turns, water also splashes over the sides into the buckets and falls from the higher buckets to lower buckets.

To make the overshoot waterwheel model more realistic, Denny[15] made a number of changes. First, real waterwheels do not have pivoted buckets. Instead, the rim of the wheel is portioned off into sections, as shown in Figure 1. They rotate with the wheel, and so water spills out increasingly as ϕ increases. Also, water splashes over the sides as it flows into the buckets. Efficiency of overshoot waterwheel model developed by Denny, as shown at equation (1)

$$\eta = \{1 + \sin(\phi)\} / \{2 + v^2 / (2 g R)\} \tag{1}$$

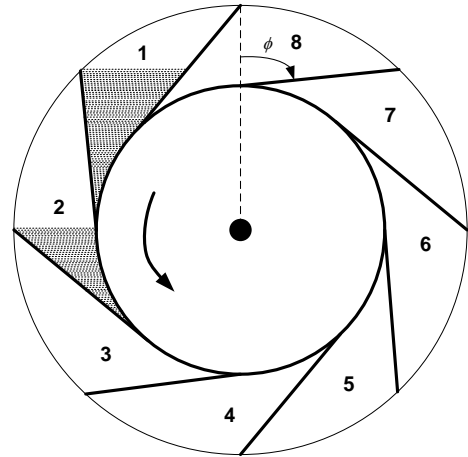


Fig.1. Overshot waterwheel with canted vanes[15]

2.2. New Model

A new design of waterwheel blade shape is changed from propeller into a triangle. The new model is compared with the previous design to show if RPM changes with the change of nozzle angle. The parameters of waterwheel include diameter, blade thickness, blade number, and length of nozzle. Water discharge was equal for all tests. The parameters of the model used were diameter = 50 cm, thickness = 10 cm, number of blades = 8, and length of nozzle = 13 cm. The design of the model can be seen in Figure 2.

The blades are attached at the edge of the wheel and installed following the line of the diameter rim. It was placed on each line in the opposite direction between the left and right side. It determines the direction of rotation of the waterwheel. Mathematical analysis of the new waterwheel model is described in more detail in section 3.

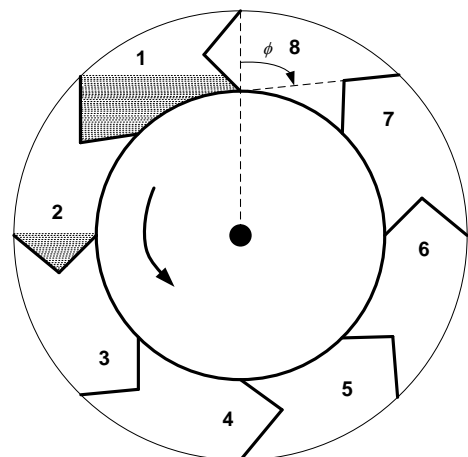


Fig.2. Design of new model waterwheels

The waterwheel model is made from acrylic material and rotates clockwise when water fills the blade. Details can be seen in Figure 3. The video demonstration of this model can be accessed at You Tube [18].



Fig.3. Model of waterwheels simulation

3. Mathematics Analysis of New Model

The waterwheel model is made in a standing position, and the blades are placed between two rims. The water is restrained on one-half of the blades, while the others are empty. Influence of earth gravitational force on the volume of water causes the wheel to spin on its axis. In this study, 16 triangular blades were attached on the edge of the wheel. The number of blades affects the simulation model, and is a consideration for the ease of construction. Our experience shows that if the waterwheel is inefficient, then water energy is not optimally converted to mechanical energy.

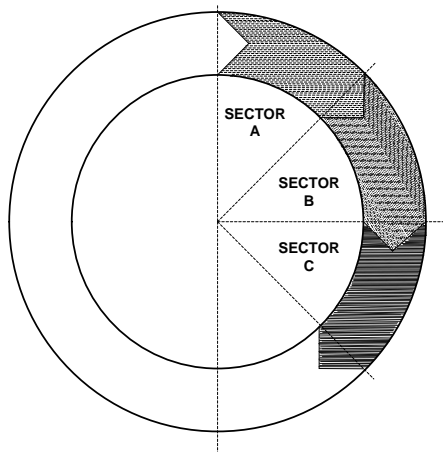


Fig.4. Sector blade of waterwheel

Water volume of each blade is calculated depending on the position of the blades on the rim while it is in motion. It is computed by multiplying surface area by thickness of wheels. With simple mathematics, the authors split the surface area of the water on each blade into three sectors. The blades positioned on the right side of the rim were divided into three sectors, namely, A, B, and C, as in Figure 4. Sector A is at an angle (α) between 0° and 45° (first quadrant includes blades 1,

2, 3, and 4). In sector A, α is the angle between vertical axis with the surface line of blade positions 1, 2, 3, and 4 on the rim. Sector B is at an angle (α) between 0° and 45° (first quadrant includes blades 5, 6, 7, and 8). In sector B, α is the angle between the horizontal axis and the surface line of blade positions 5, 6, 7, and 8 on the rim. Sector C is an angle (α) between 0° and (-45°) (fourth quadrant includes blades 9, 10, 11, and 12). In sector C, α is the angle between horizontal axis with the surface line of blade positions 9, 10, 11, and 12 on the rim.

3.1. Sector A

In Figure 5, we compute the surface area of QQXRUXQ. It is obtained by computing the surface area of triangle QXR, QQN, and RRM. Further, we compute the length of the line MN, the surface area of a triangle MNX, and the area of QQRRXQ, then the surface area of a triangle RRU and the surface area of QQXRUXQ was obtained, as shown in equation (3).

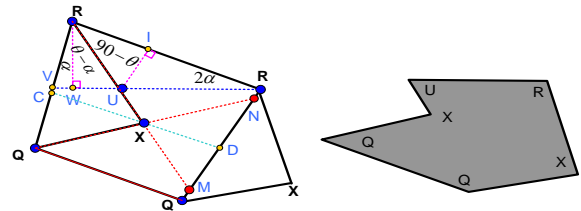


Fig.5. Surface area of sector A

Triangle QXR is computed by the following formula

$$L_{QXR} = \frac{1}{4} (QR)^2 \tan(\theta) \tag{2}$$

Area of RRU is computed as

$$L_{RRU} = \{ (PR)^2 \sin(\frac{1}{2}\alpha) [\cos(\alpha) - \cos(2\alpha) \sin(90-\alpha)] / \cos(\theta-\alpha) \} \tag{3}$$

Surface area of QQXRUXQ is equal to equation (3) minus equation (2); the result is shown in equation (4).

Surface area of QQXRUXQ =

$$A = \{ 2 \sin^2(\frac{1}{2}\alpha) \tan(90-\theta) [(PR)^2 + (PQ)^2 - \frac{1}{2} (PR+PQ)^2] \}$$

$$B = \{ \frac{1}{2} \sin(\frac{1}{2}\alpha) (PR+PQ) QR (\tan(90-\theta) \tan(\theta) + 1) \}$$

$$C = \{ \frac{1}{2} (QR)^2 \tan(\theta) \}$$

$$D = \{ (PR)^2 \sin(\frac{1}{2}\alpha) [\cos(\alpha) - \cos(2\alpha) \sin(90-\alpha)] / \cos(\theta-\alpha) \}$$

$$L_{QQXRUXQ} = [A - B + C - D] \tag{4}$$

3.2. Sector B

Figure 6 shows the computation of the surface area TQXRT. First, the triangle QXR (equation 2) and TQR are calculated. It is used to compute line TR and QS, then the surface area of triangle TQR is obtained by summing the triangle TQR and QXR, as shown by equation (7).

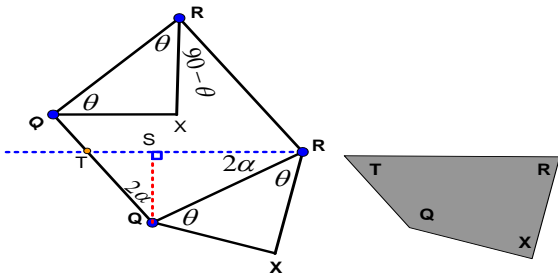


Fig.6. Surface area of sector B

Surface area of a triangle between points QRT is computed by the formula:

$$L_{QRT} = \frac{1}{2} (QR)^2 \tan(\alpha) \tag{5}$$

where the area of QXR is

$$L_{QXR} = \frac{1}{4} (QR)^2 \tan(\theta) \tag{6}$$

The surface area of TQXRT is computed with the triangles QXR and QRT, and the result is shown in equation (7)

$$L_{TQXRT} = \frac{1}{4} (QR)^2 [\tan(\theta) - 2 \tan(\alpha)] \tag{7}$$

3.3. Sector C

In Figure 7, we compute the plane area of AXR, where line AR is the surface area of the water contacting the blade. The angle BXA is represented with (beta), the angle XRQ is represented with theta, and the angle ARQ is represented with alpha; therefore, the angle XRA is represented as (theta) - (alpha). The blade angle of XRQ is equivalent to 180° - 2theta, which makes the blade an isosceles triangle. So, a triangle of XBR is a right triangle, whereby the angle of BXR is 90° - (theta - alpha).

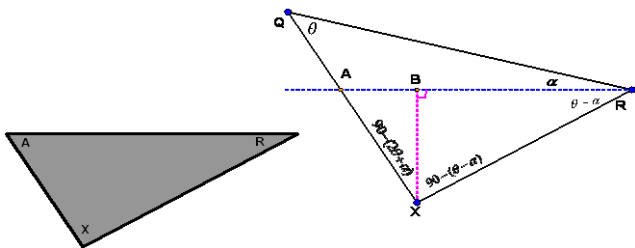


Fig.7. Surface area of sector C

Surface triangle area of AXR is computed to use a length line of RA and a height of triangle AXR. The area of triangle AXR is shown in equation (8).

$$L_{AXR} = \frac{(QR)^2 \{ \sin^2(\theta - \alpha) \tan(\beta) + \sin(\theta - \alpha) \cos(\theta - \alpha) \}}{8 \cos^2(\theta)} \tag{8}$$

4. Result and Discussion

4.1. Volume Blade Calculation

4.1.1. Simulation result

Applying equations (4), (7), and (8), the surface area of each blade is computed using Matlab simulation. When compared with previous research results[15], this study more clearly shows the volume of each blade and inference during blade movement at various angles (alpha). If the distribution of water on each blade is known, then a moment of inertia of each blade can be calculated. This result shows the influence of water mass inside the blade that causes the waterwheel to spin.

4.1.2. Experiment result

To test the validity of equations (4), (7) and (8), we compared the calculated results with manual measurements. The process measurement is performed in the laboratory of FMIPA Chemistry ITS Surabaya using a cup of 100 ml PYREX brand IWAKI ±0.5 ml, whereby it is recorded when a cup of water enters the blade. Similar steps are completed on blades 2–12. The results of the experiment can be seen in Figure 8.

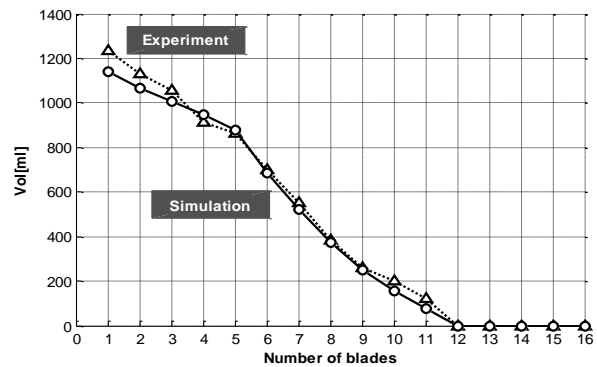


Fig.8. Relationship volume and the number of blades

4.2. Obtaining the highest RPM by experiments

4.2.1. Nozzle length

During the experiment the nozzle length was varied, and effect on the waterwheel was measured in RPM. The nozzle is made of 1/2-inch-diameter-PVC pipe with lengths including 3, 5, 8, 10 and 12 cm. The position of the nozzle upon the blade was at angles (alpha) of 0°, 11.25°, 22.5°, 45°, 56.25°, 67.5°, 78.75°, 90°, 101.25°, and 112.5° with the angle between blades being 11.25°. Measurement RPM of the turbine uses tachometer. It is placed on the horizontal axis of the waterwheels. The experiment shows that a shorter nozzle will result in a higher RPM. The highest RPM measurement obtained was seen when the nozzle angle position was 56.25° (blade 6) is 68.3. This is one adjustment that may increase the efficiency of the turbine.

4.2.2. Nozzle angle direction

Nozzle angle (alpha) direction is an angle between the nozzle and a vertical axis can be seen in Figure 9. It is always higher than the blade's position, because water fills the blades.

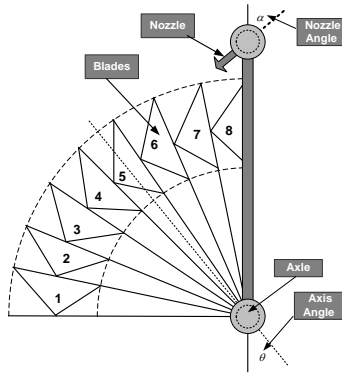


Fig.9. Position of theta and alpha angle.

The process is done with a nozzle in a fixed position on the blades; the direction of the nozzle is then adjusted from an angle 0° to the angle at which water comes out of the rim (the waterwheel is not turning). The direction of the nozzle is adjusted, and then the RPM of the wheel is measured and recorded. The analysis shows that the same angle position of nozzle and blades results in greater RPM compared to a perpendicular position. The largest RPM of the waterwheels occurs when the blade angle is approximately 40.4° .

4.3. Comparison with the new model

This author makes two model waterwheels from acrylic material with equal size where one of the blades is shaped like a propeller (model A) and the other is shaped like a triangle (model B). The RPM of the waterwheels is measured with a tachometer. The RPM values are recorded at various positions (i.e., nozzle angles). Each waterwheel consists of eight blades, as compared to the mathematical analysis that evaluates waterwheels with 16 blades.

The experiment is performed at angles of 0° and the nozzle angle adjusted from 0° to 60° . The nozzle angle (α) of model A is adjusted from 0° to 25° , but the nozzle angle in model B ranges from 0° to 22.5° . The maximum RPM of model A is 158.18 with a nozzle angle of 20° . The maximum RPM of model B is 200.80 with a nozzle angle of 17.5° . This result shows that the model B waterwheel moves 35% faster than the model A waterwheel. Figure 10 shows the RPM of model A versus model B.

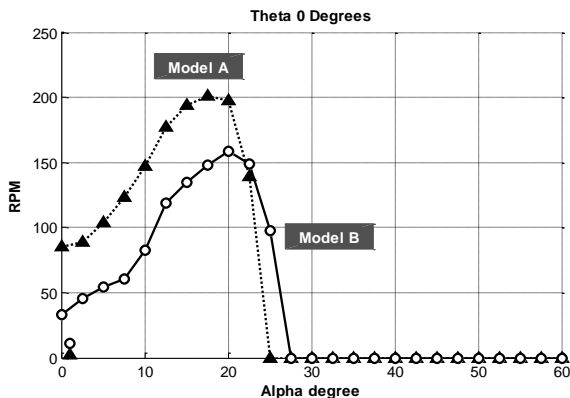


Fig.10. RPM of model A higher than that of model B.

The next step is to compare the RPM of model A to model B at angles of 5° and 10° . The maximum RPM of model A

was at 124.85 and 170.28 with nozzle angles of 20° . Model B RPM was 182.95 and 194.70 with angles of 17.5° and 15° . This result shows that the RPM of model A was lower than that of B by approximately 50% and 13.4%, respectively.

The same comparisons were made for an angle axis (θ) of 15° , 20° , and 40° , which resulted in model A being nearly equivalent to model B. The maximum RPM of model A was 224.52, 222.08, and 201.97, whereas the RPM of model B was 215.58, 213.58 and 204.025. Figure 11 shows the RPM of model A versus model B.

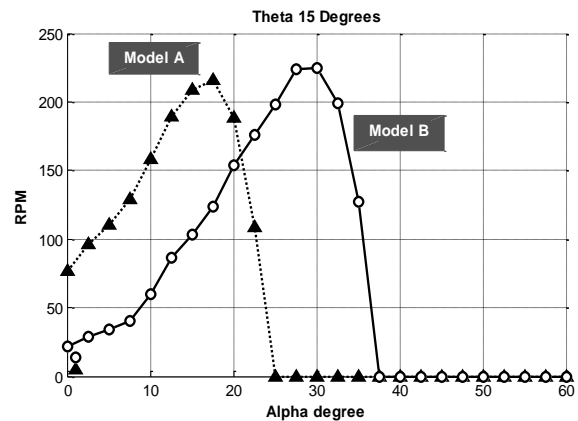


Fig.11. RPM of model A equal model B.

The same experiment for an angle axis of 35° resulted in model A being faster than model B. Maximum RPM of model A was 193.1, whereas the maximum RPM of model B was 152.68. Figure 12 shows the RPM of model A as compared to model B.

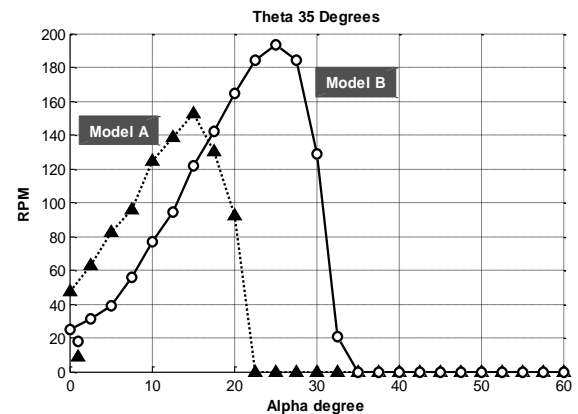


Fig.12. RPM of model A lower than that of model B

Having obtained the RPM ratio because of changes in nozzle angle and axis, we can find the value of the efficiency of the waterwheel. The value of the efficiency is calculated by comparing the output power with input power. The input power is calculated from the energy of water entering the turbine. The output power is calculated from the value of measuring currents and voltages on the generator. The results of measurements of current (I) and voltage (V), and the results of the calculation of power (P) and efficiency (η) is shown in Table 1.

Table 1. Comparison all of angle (θ) model A and model B

| Angle (θ°) | Model A (Propeller) | | | | | | Model B (Triangle) | | | | | | (η) efficiency status |
|--------------------------|----------------------------|-------|-------|-------|---------------------------|---------|----------------------------|-------|-------|-------|---------------------------|---------|----------------------------|
| | Optimal (α°) | I (A) | V (V) | P (W) | η (%) | RPM Max | Optimal (α°) | I (A) | V (V) | P (W) | η (%) | RPM Max | |
| 0 | 22,5 | 0,20 | 2,35 | 0,46 | 14,60 | 131,90 | 22,5 | 0,15 | 1,30 | 0,19 | 6,00 | 81,00 | A>B |
| 5 | 20 | 0,19 | 2,30 | 0,44 | 13,92 | 133,30 | 22,5 | 0,17 | 1,80 | 0,31 | 9,75 | 106,80 | A>B |
| 10 | 20 | 0,20 | 2,35 | 0,46 | 14,60^{*)} | 131,10 | 20 | 0,16 | 1,65 | 0,26 | 8,41 | 95,10 | A>B |
| 15 | 30 | 0,19 | 2,40 | 0,44 | 14,14 | 132,30 | 20 | 0,18 | 2,40 | 0,44 | 13,91 | 130,90 | A=B |
| 20 | 20 | 0,19 | 2,30 | 0,43 | 13,70 | 129,20 | 20 | 0,21 | 2,60 | 0,53 | 16,98 | 138,60 | A<B |
| 25 | 17,5 | 0,19 | 2,25 | 0,42 | 13,26 | 131,10 | 20 | 0,21 | 2,65 | 0,54 | 17,31 | 141,60 | A<B |
| 30 | 17,5 | 0,19 | 2,40 | 0,46 | 14,53 | 132,40 | 20 | 0,18 | 2,05 | 0,36 | 11,43 | 117,30 | A>B |
| 35 | 17,5 | 0,18 | 2,10 | 0,37 | 11,71 | 120,60 | 20 | 0,22 | 2,90 | 0,64 | 20,32^{*)} | 161,70 | A<B |
| 40 | 17,5 | 0,17 | 1,85 | 0,31 | 10,02 | 107,30 | 20 | 0,21 | 2,80 | 0,57 | 18,28 | 150,80 | A<B |
| 45 | 17,5 | 0,18 | 2,10 | 0,37 | 11,71 | 121,60 | 20 | 0,18 | 2,35 | 0,43 | 13,70 | 126,00 | A<B |

**) Maximum of efficiency*

Figure 13 and Figure 14 respectively show the resulting of RPM waterwheel based on changes in nozzle angle (α) and axis angle (θ) for models A and Model B. The maximum RPM of Waterwheel triangle Model higher than the propeller model.

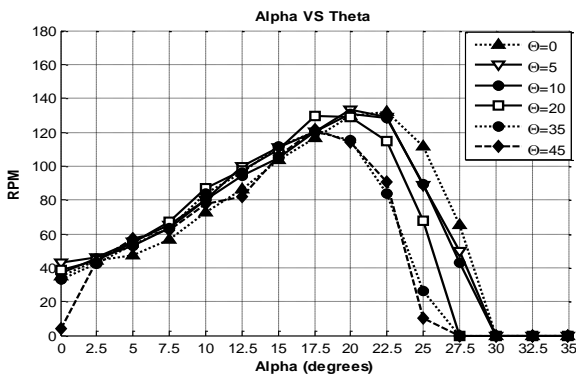


Fig.13. RPM of model A base on nozzle angle (α)

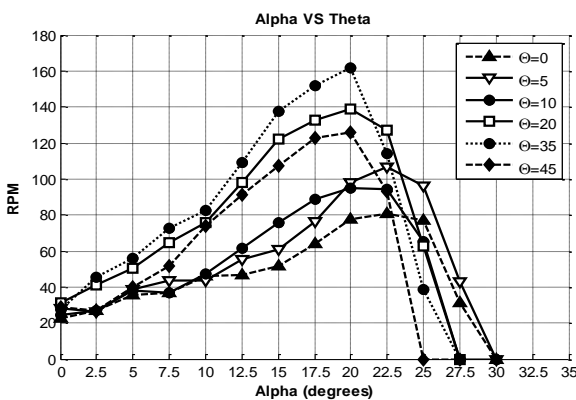


Fig.14. RPM of model B base on nozzle angle (α)

The total extractable hydraulic power from the flowing water is given by the following expression: $P_{in} = \rho g Q H$. Where P_{in} is the hydraulic power input to the wheel (W), ρ is the density of water (1.000 kg/m^3), g is the acceleration due to gravity ($9,81 \text{ m/s}^2$), Q is the volumetric water flow rate ($0,00064 \text{ m}^3/\text{s}$), H is the difference in line upstream and

downstream of the wheel = $0,5\text{m}$. P_{in} is calculated (3.14 W). $P_{out} = V I$. Where P_{out} is power output of small generator (W), V is the measurement voltage (V) and I is the measurement current of the circuit (A). The Efficiency is following expression: $\eta = P_{out} / P_{in}$. The comparison of power output for all axis angles between model A and B is shown in Figure 15.

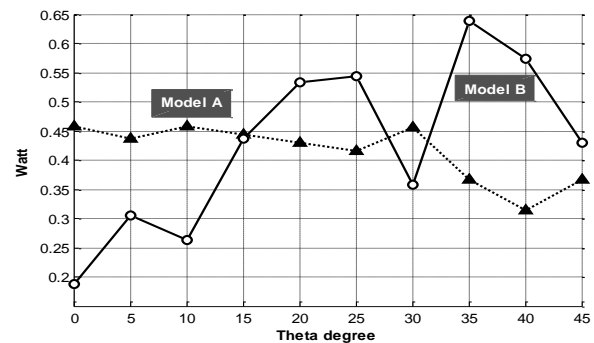


Fig.15. Power output of model A versus model B

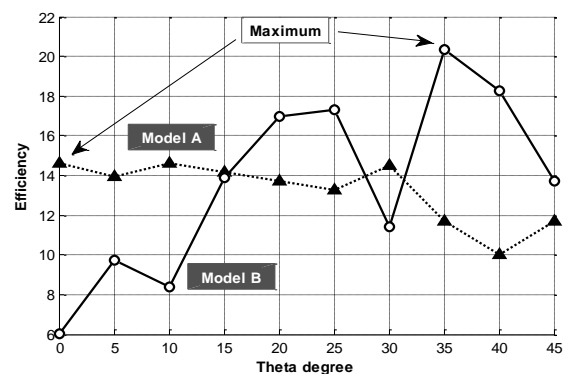


Fig.16. Efficiency of model A versus model B

The experimental results show that the maximum efficiency of model A is approximately 14.60 at $\theta = 10^\circ$, whereas in model B the maximum efficiency is approximately 20.32 at $\theta = 35^\circ$. The Efficiency of model A was lower than that of model B at $\theta = 20^\circ, 25^\circ, 35^\circ, 40^\circ,$ and 45° , but at $\theta = 0^\circ$,

5°, 10°, 15°, and 30°, the RPM of model A was higher than that of model B.

In Figure 16 is shown that the efficiency of the model A higher than model B at an angle theta 0° until 15°. At this point the water on the blades is able to optimally convert into energy. Indeed, the energy is not so great because of it resulted from the influence of the mass of water and gravity. This is evidenced when the angle theta increases, the energy produced on the wane.

5. Conclusion

Based on the section 4.1.2 above is found that the actual volume of water attached to the waterwheel is 5.36 times the volume of the blade. The capacity of water in the waterwheel can be increased by increasing the width of the waterwheel linearly, assuming that water flow is constant.

Rotation of the waterwheel is affected by the length of nozzle, with a shorter nozzle producing higher RPM. This shows that the coefficient of the nozzle used affects the RPM. Base on the section 4.2.1 above is found that the highest RPM measurement obtained was seen when the nozzle angle position was 56.25° is 68.3.

Waterwheels with triangular blades produce higher RPM than waterwheels with propeller-type blades, because the volume of water retained in the triangular blade is higher than the volume retained by a propeller blade. The mass of water in the waterwheel produced the moment inertia and then produced higher angular velocity, which caused the waterwheel to spin faster.

Nozzle angle 20° is optimal to produce the highest efficiency for waterwheel propeller and triangle. While the optimal axis angle, found respectively for the propeller 10° and 20° triangle. With axis angle of 15° will produce the same RPM.

Acknowledgements

The authors convey their greatest gratitude to the Ministry of Culture and Education, Indonesia, which provided scholarships through the Sandwich-like program 2013 at Hiroshima University, Japan.

References

- [1] T. Sakurai, H. Funato, and S. Ogasawara, "Fundamental characteristics of test facility for micro hydroelectric power generation system," presented at the International Conference on Electrical Machines and Systems, 2009. ICEMS 2009, 2009, pp. 1–6.
- [2] M. Djiteng, *Pembangkitan Energi Listrik*. Jakarta: Erlangga, 2005.
- [3] S. Paudel, N. Linton, U. C. E. Zanke, and N. Saenger, "Experimental investigation on the effect of channel width on flexible rubber blade water wheel performance," *Renew. Energy*, vol. 52, pp. 1–7, Apr. 2013.
- [4] A. Prayitno, A. Awaluddin, and A. Anhar, "Renewable energy mapping at Riau Province: Promoting Energy Diversification for sustainable development (a case study)," presented at the 2010 Proceedings of the International Conference on Energy and Sustainable Development: Issues and Strategies (ESD), 2010, pp. 1–4.
- [5] L. Wang, D.-J. Lee, J.-H. Liu, Z.-Z. Chen, Z.-Y. Kuo, H.-Y. Jang, J.-J. You, J.-T. Tsai, M.-H. Tsai, W.-T. Lin, and Y.-J. Lee, "Installation and practical operation of the first micro hydro power system in Taiwan using irrigation water in an agriculture canal," in *2008 IEEE Power and Energy Society General Meeting - Conversion and Delivery of Electrical Energy in the 21st Century*, 2008, pp. 1–6.
- [6] L. Jasa, P. Ardana, and I. N. Setiawan, "Usaha Mengatasi Krisis Energi Dengan Memanfaatkan Aliran Pangkung Sebagai Sumber Pembangkit Listrik Alternatif Bagi Masyarakat Dusun Gambuk –Pupuan-Tabanan," in *Proceeding Seminar Nasional Teknologi Industri XV*, ITS, Surabaya, 2011, pp. B0377–B0384.
- [7] L. Jasa, A. Priyadi, and M. H. Purnomo, "Designing angle bowl of turbine for Micro-hydro at tropical area," in *2012 International Conference on Condition Monitoring and Diagnosis (CMD)*, Sept., pp. 882–885.
- [8] L. Jasa, A. Priyadi, and M. H. Purnomo, "PID Control for Micro-Hydro Power Plants based on Neural Network," 2012.
- [9] L. Jasa, *Renewable Energy*. Youtube : Gambuk, Pupuan, Tabanan Bali, 2011.
- [10] A. Zaman and T. Khan, "Design of a Water Wheel For a Low Head Micro Hydropower System," *Journal Basic Science And Technology*, vol. 1(3), pp. 1–6, 2012.
- [11] G. Muller, *Water Wheels as a Power Source*. 1899.
- [12] C. A. Mockmore and F. Merryfield, "The Banki Water Turbine," *Bull. Ser. No25*, Feb. 1949.
- [13] L. A. HAIMERL, "The Cross-Flow Turbine."
- [14] J. Senior, N. Saenger, and G. Muller, "New hydropower converters for very low-head differences," vol. 48, no. 6, pp. 703–714, 2010.
- [15] M. Denny, "The Efficiency of Overshot and Undershot Waterwheels," *Eur. J. Phys.*, vol. 25, pp. 193–202, 2003.
- [16] M. Hauck, A. Rumeau, I. Munteanu, A. I. Bratcu, S. Bacha, D. Roye, and A. Hably, "A 1:1 prototype of power generation system based upon cross-flow water turbines," in *2012 IEEE International Symposium on Industrial Electronics (ISIE)*, 2012, pp. 1414–1418.
- [17] I. Vojtko, V. Fecova, M. Kocisko, and J. Novak-Marcincin, "Proposal of construction and analysis of turbine blades," in *2012 4th IEEE International Symposium on Logistics and Industrial Informatics (LINDI)*, 2012, pp. 75–80.
- [18] L. Jasa, *Model Moni Hydro*. Youtube : Denpasar, Bali, 2012.